

See discussions, stats, and author profiles for this publication at: <https://www.researchgate.net/publication/339309997>

# Four-class urine microscopic recognition system through image processing using artificial neural network

Article · January 2019

CITATIONS

9

READS

628

7 authors, including:



[Edmon Fernandez](#)

Mapúa Institute of Technology

24 PUBLICATIONS 148 CITATIONS

[SEE PROFILE](#)



[Jessica Velasco](#)

Technological University of the Philippines

41 PUBLICATIONS 415 CITATIONS

[SEE PROFILE](#)



[Migelle Jose Barlis](#)

De La Salle University

1 PUBLICATION 9 CITATIONS

[SEE PROFILE](#)

# Four-class urine microscopic recognition system through image processing using artificial neural network

Edmon Fernandez\*, Jessica Velasco, Migelle Jose Barlis, Karen Andrea Dematera, Geoferey Ilas, Rica Mae Paeste and Donnalou Taveso

Technological University of the Philippines-Manila  
Manila, Philippines

\*edmon\_fernandez@tup.edu.ph

## Abstract

Cell appearance in urine sediment is important to detect serious renal and urinary tract diseases. In this paper, digital image processing technique was efficiently used to identify and count the four most common microscopic urine constituents in the urinalysis examination: (1) white blood cells (WBC), (2) red blood cells (RBC), (3) bacteria, and (4) calcium oxalates ( $\text{CaC}_2\text{O}_4$ ). The system's structure is comprised of six sections namely, urine collection, centrifugation, image acquisition, image processing, training system, and results. The Artificial Neural Network was applied in this study for its features that can easily discern and detect urine constituents within a noisy background. The total number of image samples of WBC, RBC, bacteria, and  $\text{CaC}_2\text{O}_4$  used to train the artificial neural network are 944 with 1108 Regions of Interest (ROIs), 610 with 630 ROIs, 521 with 2047 ROIs, and 539 with 1993 ROIs respectively. The result of the microscopic examination will be generated in a pdf format. Overall, this study identifies and counts the four most common urine constituents in the microscopic urinalysis namely, the WBC, RBC, bacteria, and  $\text{CaC}_2\text{O}_4$  with an accuracy of 93.70%.

**Keywords:** image processing; microscopy; neural network; urinalysis; feature extraction

## 1. Introduction

Since the 1800s, urinalysis has been part of the routine medical examination. It is an essential part of the patient's examination then until now with the continued development of modern testing techniques. Two unique characteristics of urine made it well-known in the field of medicine. The first being urine is readily available and an easily collected specimen and the second being urine reveals information about the body's major metabolic functions which can be obtained by inexpensive laboratory [1].

According to the Clinical and Laboratory Standards Institute (CLSI), urine testing is usually done in an efficient, fast, reliable, accurate, safe, and cost-effective manner. Also, it is normally performed to aid medical doctors for diagnosis of certain disorders, screening asymptomatic people for undetected illness, and monitoring the progress of disease or the effectiveness of medication [1]. Results in a urinalysis examination are commonly correlated to a patient's physical symptoms to further verify disease identification.

Urinalysis is composed of three parts: the physical, chemical, and microscopic examination. Microscopic urinalysis enables medical technicians to detect the presence of components that often gives early diagnostic information concerning dysfunction, infection, or inflammation of the kidneys and urinary [2]. Hence, clinical case management would really benefit in this unobtrusive technique.

However, medical technologists manually read and identify samples visually in the traditional manual microscopic analysis. This routine manual analysis results to some significant cell count discrepancies and sometimes error. As a result, urinalysis has become relatively tedious and hard to standardize. Automated microscopy eliminates the variation among technologists and consequently make it more practical. Since this traditional method is labor-intensive for oper-

ators, automatic urine sediment analyzer becomes a necessity [3].

Two automated urine cell analyzers are currently available in the United States: the Sysmex UF-1000i and the IQ 200 from Iris Diagnostics which use laser-based flow cytometry that measures light scatters, fluorescence staining characteristics, and adaptive cells [1]. This paper presents the development of an efficient and cost-effective system that automatically recognizes and counts the WBC, RBC, bacteria, and  $\text{CaC}_2\text{O}_4$  in the urine sediments through digital image processing supported by different algorithms through Artificial Neural Network.

## 2. Methodology

The system's structure is composed of six main sections: urine collection, centrifugation, image acquisition, image processing, training system, and result as can be seen in Figure 1.

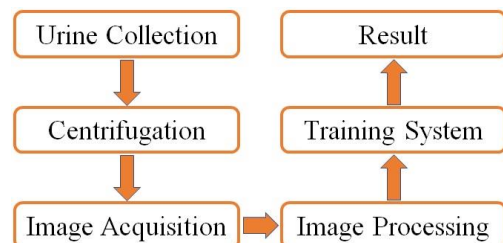


Fig. 1: System block diagram

### 2.1. Urine collection

The patient's urine is the primary input of the system. It was collected using dry, clean, and leak-proof containers as can

be seen in Figure 2a. These disposable containers are used to prevent contamination of the urine specimen. The urine sample is collected as a midstream clean-catch technique which also reduces contamination by other cells or external dirt [1].



Fig. 2: (a) Photograph of the urine container; (b) test tube

## 2.2. Centrifugation

The collected sample which is usually between 10 and 15 mL is transferred to a conical tube as seen in Figure 2b for centrifugation. This provides an acceptable amount to obtain a representative sample specimen of the elements present in the urine [1].

The specimen is centrifuged for five minutes at a relative centrifugal force (RCF) of 400. This configuration provides an optimum amount of urine sediment without damaging its elements.

The revolutions per minute (RPM) value shown on the tachometer of the centrifuge is converted to RCF using the formula in (1).

$$RCF = 1.118 \times 10^{-5} \times r \times RPM$$

**Definition 2.1:** RCF is for relative centrifugal force,  $r$  is for radius of revolution, and RPM is for revolutions per minute

## 2.3. Image acquisition

The sediment that remained after centrifugation, usually between 0.5 mL and 1.0 mL, are poured off to a microscopic slide as seen in Figure 3a with dimensions of 22 mm x 22 mm. The sediment is re-suspended on the microscopic slide to make a homogenous distribution of elements in the microscopic examination. The recommended amount of the re-suspended sediment when using the glass-slide method is about 0.02 mL [1].

The microscopic slide is placed under the microscope and set for examination. It is viewed under the high-power (40x) objective (x400 magnification) for about five microscopic fields [1].

The system is equipped with a 1.3MP microscopic camera as shown in Figure 3b. It is responsible for taking ten-image samples per microscopic field for about five fields of the sediment to cover the entire high-power field area. The number of images to be captured per field is due to the relative difference of the viewing area of the microscopic camera and the actual high-power field area.



Fig. 3: Photograph of: (a) microscopic slide; (b) microscopic camera



Fig. 4: User interface of MicroPee

Image capturing is controlled by a Graphical User Interface (GUI) which is provided using Visual Studio installed in a computer. This interface also allows the user to encode, record, and display patient's information, manually input physical, chemical and microscopic parameters, and generate results in Portable Document Format (PDF). The GUI also calls the compiled MATLAB® functions to perform recognition and counting of the cells after the captured images are already complete. A screenshot sample of the user interface is shown on Figure 4.

## 2.4. Image processing

The image processing section is subdivided into two sub-processes: image segmentation, and feature extraction. These are

### 2.4.1. Image segmentation

The region of interest (ROI) of the images acquired from the microscopic camera are cropped using the Training Image Labeler of MATLAB® R2015a. A sample of cropped ROI for each of the class is presented in Figure 5.

Here, the image processing involves leveling method to avoid detection of a single ROI. ROIs were determined by scanning every region of the image using four detectors. Successful detection of a certain region yields to the application of a mask and bypasses the other parameters and proceeds to other regions.



(a) ROIs of WBC

(b) ROI of RBC

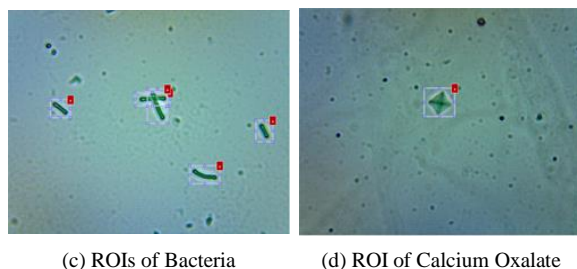


Fig. 5: Original images of cells and its ROI/s

## 2.4.2. Feature extraction

Two different features are extracted to identify the urine elements: (1) histograms of oriented gradient (HOG) of the image and; (2) local binary patterns (LBP).

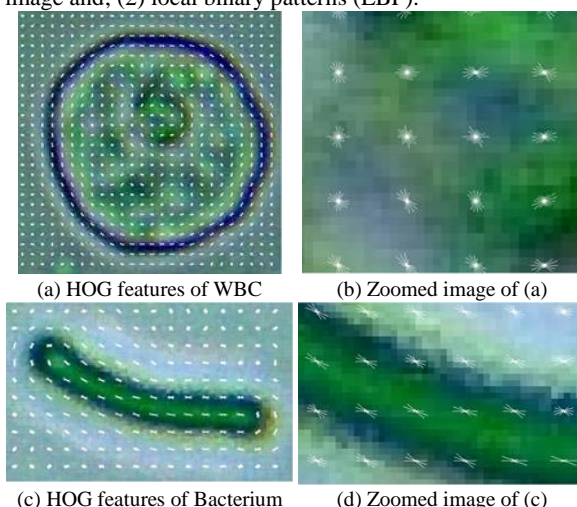


Fig. 6: HOG feature extraction results

HOG is executed by fragmenting the image into smaller cell parts, for each cell part accumulating a local 1-D histogram of edge orientations over the pixels of the cell. The combined histogram entries form the representation [3]. Two samples of HOG implementation for WBC and bacterium are presented in Figure 6.

LBP, on the other hand, is a texture operator which marks the pixels of an image by thresholding the neighborhood of each pixel and considers the result as a binary number [4]. LBP implementation samples for both WBC and Calcium Oxalate are presented in Figure 7 including its histogram.

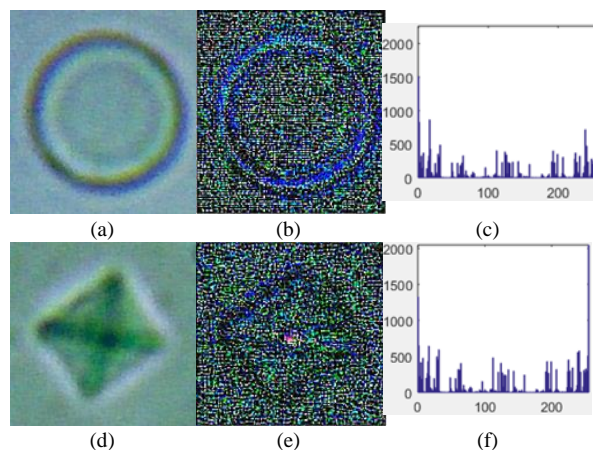


Fig. 7: LBP feature extraction results: (a) Original image of RBC; (b) LBP image of RBC; (c) LBP histogram of RBC; (d) Original Image of  $\text{CaC}_2\text{O}_4$ ; (e) LBP Image of  $\text{CaC}_2\text{O}_4$ ; and (f) LBP Histogram of  $\text{CaC}_2\text{O}_4$

## 2.5. Training system

The processed images are used as input for training the system. The samples used in training the system were screened by medical technicians to ensure the reliability of the neural network.

The system is trained using the backpropagation neural network architecture via cascade object identifier of MATLAB® to improve the accuracy.


The database of the neural network is comprised of the ROIs of WBCs, RBCs, bacteria and  $\text{CaC}_2\text{O}_4$ , which are recorded as positive instances, and negative instances, which includes images of noise, background, and other urine constituents that are not going to be recognized. The total number of image samples of WBC, RBC, bacteria and  $\text{CaC}_2\text{O}_4$  used to train the neural network are 944 with 1108 ROIs, 610 with 630 ROIs, 521 with 2047 ROIs, and 539 with 1993 ROIs respectively.

The process of training is done by the cascade identifier tool. This allows the neural network to improve its performance and reliability by automatically adjusting the random variables added on either the histogram or binary pattern of the ROI. The training process of cascade object identifier aims to reach a maximum of 50 stage neural network at an error of 0.005.

The training system produces object detectors for WBC, RBC, bacteria and  $\text{CaC}_2\text{O}_4$  that are embedded in an xml file.

## 2.6. Result


The result section generates a pdf file as shown in Figure 8 that is composed of the system's analysis for WBC, RBC, bacteria and  $\text{CaC}_2\text{O}_4$ , and other urinalysis' parameters that are manually encoded by medical technicians. This result is presented in two different approach: (1) Quantitative result for WBC and RBC count; and (2) Qualitative result for bacteria and  $\text{CaC}_2\text{O}_4$ .



Citi\_care Ultrasound Services and Diagnostic Center

1018 National Road Binakayan, Kawit, Cavite

18, www.facebook.com/Citi\_care-Ultrasound-Services-and-Di



In Cooperation with

Micro-Pee

Citi\_care Ultrasound Services and Diagnostic Center

1018 National Road Binakayan, Kawit, Cavite


Report Date/Time:

02/09/2017 03:18:26

Name:	Pastor, Rica Mae Javier	Age:	21	Record ID:	000000002
Patient ID:	000000227	Sex:	Female	Status:	ROUTINE
Date of Birth:	8/8/1995	Civil Status:	Single	Affend Dr:	None

Test	Normal	Abnormal	Flag	Reference
URINE PHYSICAL				
URINE CHEMICAL				
GLUCOSE	NEGATIVE			NEGATIVE
BILIRUBIN		POSITIVE	H	NEGATIVE
KETONE		TRACE	H	NEGATIVE
SPECIFIC GRAVITY	1.004			1.003 - 1.035
BLOOD	NEGATIVE			NEGATIVE
PH	6.0			5.0 - 8.0
PROTEIN		NEGATIVE	H	N/A
UROBILINOGEN	0.3			0.1 - 1.0
NITRITE		POSITIVE	H	NEGATIVE
LEUKOCYTES		POSITIVE	H	NEGATIVE
URINE MICROSCOPIC				
RBC		0 - 1	H	NONE SEEN
WBC		1 - 3	H	NONE SEEN
BACTERIA	RARE			RARE
URINARY CRYSTALS				
CALCIUM OXALATE		NONE	H	NONE SEEN

Note: Please correlate laboratory results clinically for appropriate interpretation.



MICRO-PEE

PHYSICAL MEDICINE

Maldy R. Dimaculangan, RMT

Medtech

Florcita Ludviga T. Solis, MD, FSP

Pathologist

Fig. 8: Screenshot of the generated result in PDF

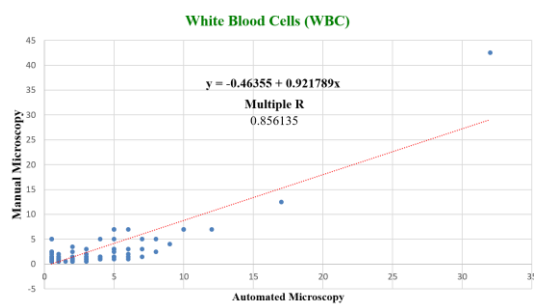


### 3. Data and results

This section comprises the data and results of the four – classes of urine obtained from 123 patients, their comparison between the automated and manual counts when grouped, and the summary of the accuracy, specificity and sensitivity of the system.

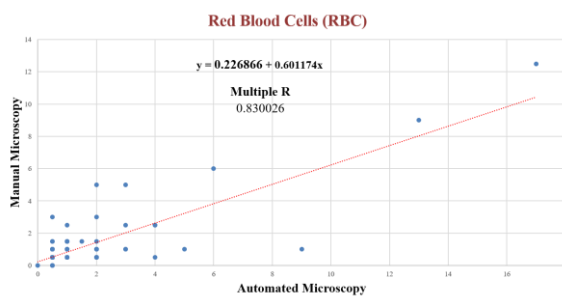
#### 3.1. Correlation results

Figure 9 shows a strong correlation between the manual and automated White Blood Cells (WBC) count with a correlation coefficient of 0.856. The t-test obtained, assuming equal variances for WBC, is  $t_{Stat} < t_{Critical}$  ( $1.345 < 1.970$ ) and  $p\text{ value} > \alpha$  ( $0.180 > 0.05$ ), which means that there is no significant difference on the means of the automated and manual results.



**Fig. 9:** Correlation between manual and automated counting for WBC

The results of the manual and automated counts for Red Blood Cells (RBC) are plotted in Figure 10, resulting in a correlation coefficient of 0.83. The t-test obtained, assuming unequal variances for RBC, is  $t_{Stat} < t_{Critical}$  ( $1.308 < 1.971$ ) and  $p\text{ value} > \alpha$  ( $0.192 > 0.05$ ), which means that there is no significant difference on the means of the automated and manual results.



**Fig. 10:** Correlation between manual and automated counting for RBC

The results of the manual and automated counts for Bacteria were plotted in Figure 11, resulting in a correlation coefficient of 0.411. The t-test obtained, assuming unequal variances for Bacteria, is  $t_{Stat} > t_{Critical}$  ( $2.672 < 1.974$ ) and  $p\text{ value} < \alpha$  ( $0.008 < 0.05$ ), which means that there is a significant difference on the means of the automated and manual results.

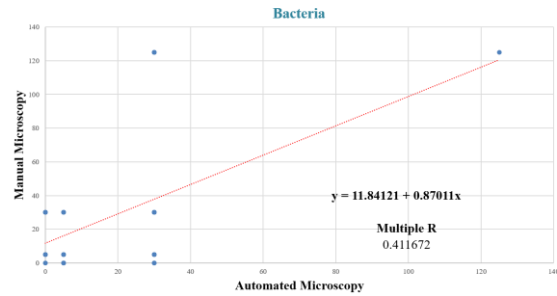


**Fig. 11:** Correlation between manual and automated counting for bacteria

Figure 12 shows the relationship between the manual and automated counts for Calcium Oxalate. It has a strong correlation coefficient of 0.947. The t-test obtained, assuming equal variances for Calcium Oxalate, is  $t_{Stat} < t_{Critical}$  ( $1.970 < 0.331$ ) and  $p\text{ value} > \alpha$  ( $0.741 > 0.05$ ), which means that there is no significant difference on the means of the automated and manual results.

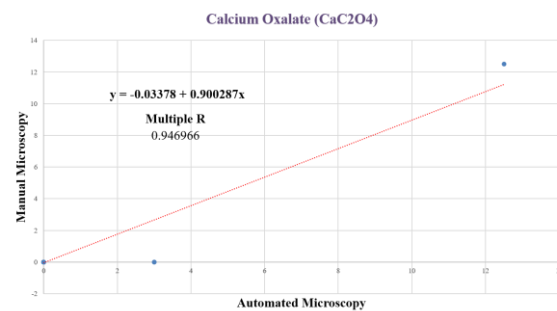


**Figure 12:** Correlation between manual versus automated counting for Calcium Oxalate ( $\text{CaC}_2\text{O}_4$ )

#### 3.2. Tabulated results

Table 1 shows that when the automated count of White Blood Cell (WBC) was grouped in similar range, 115 of 123 were within one grading difference and 123 of 123 (100%) were within two grading differences. Using the manual method of counting as a ‘gold standard’, the automated WBC count had an accuracy of 93.496%, a specificity of 95.833% and a sensitivity of 85.185%, considering a one grading difference a true value.

**Table 1:** Comparison of Automated and Manual White Blood Cell (WBC) Counts when Grouped

Manual WBC count group (/hpf)	Automated WBC count group (/hpf)						
	0 – 2	2 – 5	5 – 10	10 – 25	25 – 50	50 – 100	> 100
0 – 2	72	20	4	0	0	0	0
2 – 5	5	8	6	0	0	0	0
5 – 10	4	1	1	0	0	0	0
10 – 25	0	0	0	1	0	0	0
25 – 50	0	0	0	0	1	0	0
50 – 100	0	0	0	0	0	0	0
> 100	0	0	0	0	0	0	0

Table 2 shows that when the automated count of Red Blood Cell (RBC) was similarly grouped, 122 of 123 were within one grading difference and 123 of 123 (100%) were within

two grading differences. Using the manual count as a ‘gold standard’, the automated RBC count had an accuracy of 99.187%, a specificity of 100% and a sensitivity of 91.667%, considering a one grading difference a true value.

**Table 2:** Comparison of Automated and Manual Red Blood Cell (RBC) Counts When Grouped

Manual RBC count group (/hpf)	Automated RBC count group (/hpf)						
	0 – 2	2 – 5	5 – 10	10 – 25	25 – 50	50 – 100	> 100
0 – 2	107	4	1	0	0	0	0
2 – 5	2	6	0	0	0	0	0
5 – 10	0	0	1	1	0	0	0
10 – 25	0	7	0	1	0	0	0
25 – 50	0	0	0	0	0	0	0
50 – 100	0	0	0	0	0	0	0
> 100	0	0	0	0	0	0	0

Table 3 shows that when the automated count of Bacteria was similarly grouped, 103 of 123 were within one grading difference and 123 of 123 (100%) were within two grading differences. Using the manual count as a ‘gold standard’, the automated RBC count had an accuracy of 83.74%, a specificity of 40.741% and a sensitivity of 95.833%, considering a one grading difference a true value.

**Table 3:** Comparison of Automated and Manual Bacteria Counts When Grouped

Manual Bacteria count groups (/hpf)	Automated Bacteria count groups (/hpf)				
	0	0 – 10	10 – 50	50 – 200	> 200
0	2	9	4	0	0
0 – 10	16	11	21	0	0
10 – 50	16	7	24	0	0
50 – 200	0	0	12	1	0
> 200	0	0	0	0	0

Table 4 shows that when the automated count of Calcium Oxalate ( $\text{CaC}_2\text{O}_4$ ) was similarly grouped, 121 of 123 were within one grading difference and 123 of 123 manual count as a ‘gold standard’, the automated RBC count had an accuracy of 98.374%, a specificity of 100% and a sensitivity of 33.333%, considering a one grading difference a true value.

**Table 4:** Comparison of Automated and Manual Calcium Oxalate ( $\text{CaC}_2\text{O}_4$ ) Counts when Grouped

Manual $\text{CaC}_2\text{O}_4$ count groups (/hpf)	Automated Calcium Oxalate ( $\text{CaC}_2\text{O}_4$ ) count group (/hpf)				
	0	0 – 2	2 – 5	5 – 20	> 20
0	119	1	2	0	0
0 – 2	0	0	0	0	0
2 – 5	0	0	0	0	0
5 – 20	0	0	0	1	0
> 20	0	0	0	0	0

Table 5 shows the summary of results of accuracy, specificity and sensitivity of the recognition system for each cell. For all the four classes, the system has an average of 93.7% accuracy, 84.14% specificity, and 76.51% sensitivity.

**Table 5:** Summary of Results

	Accuracy	Specificity	Sensitivity
WBC	93.50%	95.83%	85.19%
RBC	99.19%	100%	91.67%
Bacteria	83.74%	40.74%	95.83%
Calcium Oxalate	98.37%	100%	33.33%
Total	93.70%	84.14%	76.51%

## 4. Conclusion

Based on the research results, the development of the automated urine microscopic recognition system that analyses the four cell classes such as white blood cells, red blood cells, crystals (calcium oxalate) and bacteria through image processing using artificial neural network was successfully implemented using Microsoft Visual Studio and MATLAB®.

Test results prove that this method is an effective and accurate way of recognition and counting with an accuracy of 93.7%. However, there are at least three aspects for further exploration. First, a greater number of ROIs should be added for refining the recognition capability of the system. Second, more features can be considered to increase the accuracy of the system. And lastly, automating the image acquisition part of the system which involves gears and stepper motors for achieving faster acquisition and elimination of human intervention.

## Acknowledgement

The researchers are grateful to the CITI\_CARE Ultrasound Services and Diagnostic Center and EMK Diagnostic Laboratory and X-Ray for being the partner clinical laboratories and for usage of their facilities.

## References

- [1] S. K. Strasinger, “Introduction to Urinalysis,” in *Urinalysis and Body Fluids*, 6th ed., Philadelphia, Pennsylvania: E. A. Davis Company, (2014), pp. 28-29.
- [2] C. Y. Li et al, “Automatic detection and recognition of casts in urine sediment images,” *Proceedings in Int'l. Conf. on Wavelet Analysis and Pattern Recognition*, China, (2009), <https://doi.org/10.1109/ICWAPR.2009.5207456>
- [3] M. Ranzato et. al, “Automatic recognition of biological particles in microscopic images,” *Pattern Recognition Letters*, Vol. 28, Issue 1, 1, (January 2007), pp. 31-39.
- [4] B. J. Bain, “Blood cells: a practical guide,” *Performing a Blood Count*, 4th ed., J. Wiley & Sons Inc., (October 2007), p. 28
- [5] Dalal and B. Triggs, “Histograms of oriented gradients for human detection,” *IEEE Computer Society Conference on Computer Vision and Pattern Recognition*, Vol. 1, (June 2005), pp. 886–893.
- [6] Matti Pietikäinen (2010). Local Binary Patterns. Scholarpedia, 5(3):9775. Retrieved from [http://www.scholarpedia.org/article/Local\\_Binary\\_Pattern](http://www.scholarpedia.org/article/Local_Binary_Pattern).
- [7] W. Dimech and K. Roney (2002), “Evaluation of an automated urinalysis system for testing urine chemistry, microscopy and culture,” *Pathology*, Vol. 34, pp. 170-177.